Modified Slip Coupling Design for High Temperature Conditions in HTGRs

Sweejal Kafle, Nathalie Schelin, Mariam Lara, Elizabeth Wells, and Bryan Kuhr*
*Corresponding Author: bkuhr@sbc.edu

The Margaret Wyllie Engineering Program
Sweet Briar College
Sweet Briar, VA, USA

***Abstract*—High-temperature gas-cooled nuclear reactors (HTGRs) are Generation IV reactors currently in development around the world that can provide efficient electricity generation and industrial heat. However, their high coolant temperatures also drive significant thermal expansion in coolant piping, which in turn creates high piping stresses and a need for expansion joints that accommodate large axial movements while maintaining the coolant pressure boundary. This project aims to develop a coupling to accommodate 4 to 6 inches of axial growth in HTGR coolant piping while withstanding internal pressures from 5 torr vacuum to 4.8 MPa internal pressure at temperatures reaching 900°C. Conventional expansion loops, bellows joints, and slip joints are challenged under these conditions. To improve flow characteristics and service life while meeting the operating requirements of the HTGR environment, the selected solution is a modified slip coupling with three key features: external pressurization to improve pressure and temperature performance of sealing, springs for thrust-load dissipation, and metallic seals instead of more temperature-limited packing materials. This design is evaluated using finite element analysis and requirements from ASME B31.1, B31.3, and BPVC Section VIII Division 2 for protection against collapse and failure from cyclic loading. The resulting design balances axial motion, pressure retention under high temperatures, leakage reduction, and maintainability, providing a practical solution for HTGR piping systems.**

Keywords—Nuclear, Piping, Expansion Joints

I. INTRODUCTION

High-temperature gas-cooled reactors, commonly referred to as HTGRs, are Generation IV reactors that use high-temperature gas (typically helium) as a primary coolant, with outlet temperatures reaching 700°C or higher [1]. Fig. 1 shows an example schematic of an HTGR system. BWXT is working to design a range of reactor designs for space, fixed base and mobile applications all using HTGR technology. BWXT's mobile microreactors application introduces additional constraints to meet portability and size constraints. The goal of this project is to address one such technical challenge with HTGRs in this environment: how to accommodate large axial thermal expansion in primary coolant piping using a compact system appropriate for a microreactor.

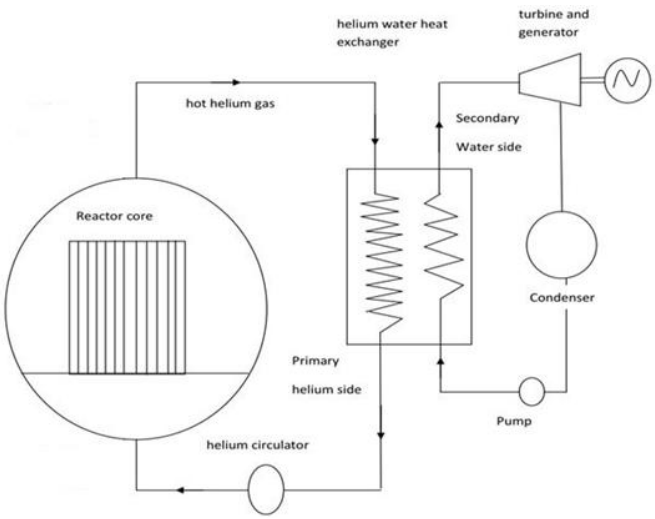

Fig. 1. HTGR system with helium used as a coolant gas [2]

Thermal expansion in piping follows:

$$\Delta L = L\alpha\Delta T \tag{1}$$

Here, L is the original pipe length, α is the coefficient of thermal expansion (CTE) for the material, and ΔT is the change in temperature [3].

Due to high HTGR operating temperatures, a single pipe run can grow several inches axially. If that growth is not accommodated, the resulting forces build up in the piping system and risk pressure boundary failure. For BWXT's application, a coupling must be designed to accommodate movement of 4 to 6 inches axially while also withstanding operating conditions ranging from a 5 torr vacuum during start-up to 4.8 MPa and 900°C at full operation. The leakage of the gas coolant should be held below 1 g/day over a three to five-year service life, since coolant loss adds cost and burden to the system and could become a safety and environmental hazard if contamination occurred. Four candidate designs were identified

and evaluated: expansion loops, bellow joints, ball joint couplings, and slip couplings.

Expansion loops use U- or Z- shaped pipe bends to absorb thermal growth by flexing the pipe itself, with no moving parts or seals involved (see Fig. 2). They are the simplest available design of expansion joints and can be ideal for applications where minimizing piping dimensions or pressure drop is not a priority.

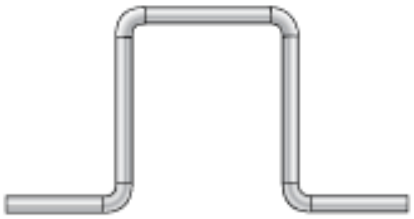

Fig. 2. Expansion loop [4]

While expansion loops function well in large industrial piping systems where space is not a constraint, space is critical in applications like those in BWXT's microreactor designs. A loop absorbing four to six inches of axial growth would require a large assembly, inappropriate for a microreactor design. Each additional elbow also introduces additional pressure losses, increasing the pressure drop across the system [5]. Increasing pressure drop reduces coolant flow or requires the use of more powerful pumps or compressors, which decreases efficiency.

Bellows joints take a more compact approach, using thin-walled corrugated metal elements that compress and extend as the surrounding piping moves (see Fig. 3).

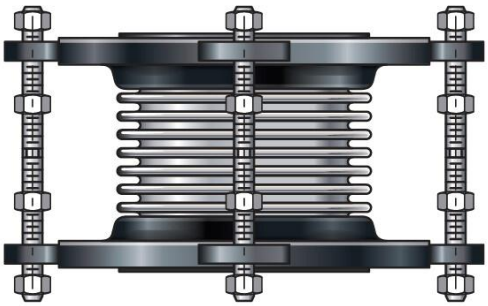

Fig. 3. Bellows joint [6]

They can contain high system pressures and accommodate axial, angular, and lateral movement, but their corrugations are susceptible to fatigue under repeated mechanical and thermal cycling. Once a bellows section has degraded, the only maintenance option is full replacement [7]. Like expansion loops, bellows joints cause significant pressure drops.

Ball joint couplings (Fig. 4) allow angular rotation and some axial accommodation through a spherical ball-and-socket interface sealed with a packing material. Commercially available designs use seals rated to only 540°C, well below the 900°C requirement. When multiple ball joints are used in series to handle axial movements, each joint also becomes an additional potential leak point [8].

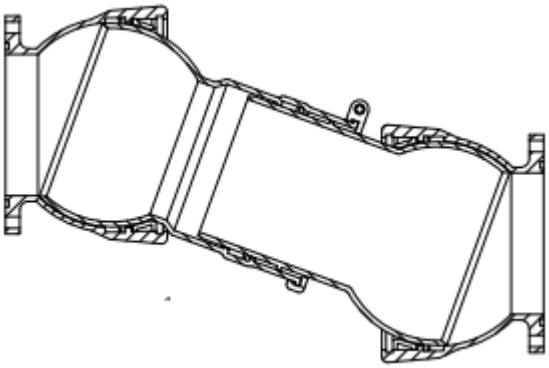

Fig. 4. Ball Joint Couplings [9]

Slip couplings (Fig. 5) operate on a simpler principle: an inner pipe slides within an outer sleeve as the surrounding piping expands axially. This type of coupling accommodates axial displacements without introducing bending fatigue or multiplying leak paths. This type of coupling also uses packing materials, similar to the ball joint couplings [10]. The limitation of slip couplings is that conventional packing materials, graphite and PTFE, are rated to 650°C and 260°C respectively, neither of which meets the operating requirements of HTGRs [11].

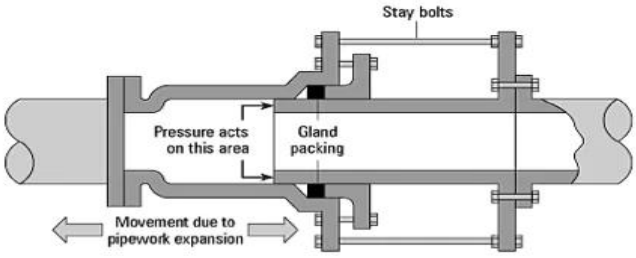

Fig. 5. Slip Coupling [12]

During concept selection, the team prioritized simplicity, flow characteristics, and longevity at high temperature and pressure. Hence, the slip coupling was selected as the design baseline. Unlike the fatigue-driven failure mode of bellows or the complexity of ball joints, the slip coupling's primary limitation is one that can be addressed through targeted modifications: particularly, packing material performance. The design developed for this project incorporates three such modifications. First, an external pressurization element

improves leakage performance at the pressure-temperature interface. Second, metallic seals replace traditional packing materials. Lastly, springs dissipate the axial thrust loads the coupling would otherwise transmit into adjacent pipe supports. The sections that follow describe the design, analysis and iterative development of this modified slip coupling in detail.

II. Methods And Materials

The design and sizing of the coupling were guided by ASME code. ASME B31.1 and B31.3, Power Piping and Process Piping, were the governing standards for the design. Since the coupling would be a first-of-a-kind component, ASME BPVC Section VIII Division 2 provided the basis for the design through analysis. Haynes 230, a nickel-based superalloy, was selected as the primary structural alloy for the coupling based on its high-temperature mechanical capability and established use in elevated-temperature service. The initial design concept was developed from an existing slip coupling architecture, with a rough sketch used to establish the geometry before transitioning to parametric modeling in Autodesk Inventor. Pipe sizing followed standard schedule dimensions, and components such as flanges and metallic seal rings were dimensioned from manufacturer and industry standard references [15]. The outer coupling was sized to interface with a 10 NPS inner diameter. The inner pipe is structured to have a 1-inch wall thickness (nominally Schedule 160) to withstand 700 psi at 900°C. Unlike the previous adoption of SI units, the team decided to continue the project from this point to the USCS unit system to be consistent with NPS standards. To facilitate axial movement, the outer sleeve features an inner diameter of 10.980 inch and an outer diameter of 13.480 inch which expands to a 14.980-inch diameter weld neck pipe-end [16], providing a 0.230-inch diametrical clearance. Modified 2-inch-thick Class 900 flanges [17] with an expanded 27.4-inch diameter on both ends of the coupling are used to connect the coupling to the surrounding piping. Circular lugs are bolted to the flanges to support springs and tie-rods outside the primary pressure boundary, preventing overextension, torsion, or excessive thrust loads.

The metallic seals are designed to grow toward the inner pipe as the coupling heats to its operating temperature. The seal material selection required careful consideration of thermal expansion compatibility. Initial calculations using 316H stainless steel introduced a fundamental problem: working backwards from a target interference of 0.001 inch at 900°C produced a negative clearance at cold assembly, meaning the ring could not be installed over the pipe at room temperature without interfering with the pipe. Matching the seal material to the pipe (Haynes 230 on Haynes 230) maintained tight interference at hot temperature, but the seal would still need to be assembled with some contact with the pipe at cold temperature. The team explored various other candidates such as Inconel 718, Inconel 600, and Inconel 601, which did not meet the design requirements due to their Cobalt and Tantalum composition, both of which were restricted for this application. The team thus considered other alloys with lower CTE values, out of which Titanium-Zirconium-Molybdenum alloy (TZM alloy: Mo-0.5Ti-0.1Zr) was the best contender with a CTE value: 5.45×10^{-6} /°C [18], less than half that of Haynes 230. This low thermal expansion rate allows the seal to start with positive clearance at assembly and develop interference as the faster-expanding Haynes 230 pipe grows into it at operating temperature. TZM also provides high-temperature strength exceeding 1300°C and contains no cobalt and tantalum [19].

Seal dimensions were determined by working backwards from the operating condition. The radial height of 0.350 inch was taken from a metallic ring seal catalog for the applicable bore size. A target interference of 0.001 inch at the inner sealing interface was selected at 900°C with installation temperature at 25°C. The required seal inner radius was calculated to be 5.4225 inch, and the seal outer radius to be 5.7725 inch. The groove in the outer pipe was sized to accommodate the seal at maximum thermal expansion, giving a depth of 0.287 inch and an axial width of 0.389 inch. At 900°C, the seal maintains 0.001 inch of interference against the inner pipe surface, hence acting as a tight sealing interface. At the assembly temperature, the seal requires a cold clearance between the ring ID (10.845 inch) and pipe OD (10.750 inch) to be 0.095 inches in order to close to the target interference at operating temperature.

The design process followed an iterative workflow in which geometry updates, stress analysis and design review were conducted in sequence, with each FEA result informing the next geometric iteration.

III. Results

A. Modeling

The coupling design was developed across ten iterative revisions in Autodesk Inventor. Early iterations established the overall slip coupling structure and primary pressure boundary dimensions. Initial versions of the iterative process use a two-part modified slip coupling structure and was based upon the model in Fig. 6, while later iterations use a three-part slip coupling design [20].

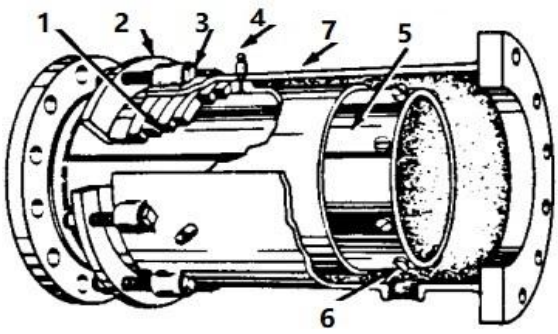

Fig. 6. Slip Coupling Base Structure [20]

Incorporated in these early iterations was a modified version of the bumper feature of Fig. 6. The bumper is shown with the number 6 label pointing to that feature [20]. The team also worked to incorporate springs. Springs were explored as a way to accommodate for thrust loads presented under the

extreme pressure and temperature environment of the system. Throughout the design process, subsequent revisions worked on refining certain dimensions, such as the wall thickness, to incorporate a better design based upon the analysis results. In the later revisions, a three-part model was explored to lessen the fatigue and overextension of the springs in the system. Tie rods were incorporated to reinforce the model's stability and fatigue on the springs. A simplified picture of this model is shown below in Fig. 7.

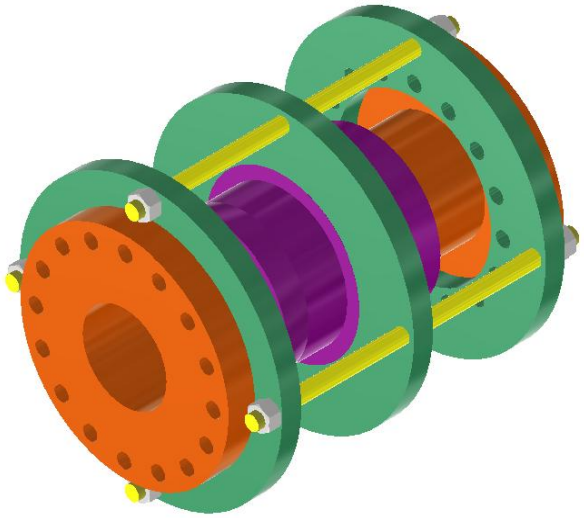

Fig. 7. Final Three-Part

Throughout the iterative process, the details on the seals were refined as well as the springs. In the last iteration, the springs requirements were specified and seals were completed. The team ultimately chose to select the three-part model, given its internal profile could produce a lower pressure drop than the two-part version.

Three spring types were evaluated to find a design that could resist approximately 2×10^5 Newtons of thrust load across the coupling body, accommodating 2 inches of axial movement. The design plan was to place four spring sets in parallel with each other, with each set containing two springs put on either side of the central circular lug (see Fig. 7). Helical coil springs were ruled out because achieving four to six inches of deflection while maintaining a large enough axial load capacity required wire diameters which were impractically large. Wave springs also could not carry the required load within the available diameter range although they were a better candidate than traditional helical springs in terms of radial space. These springs were also found to exceed the allowable stress limit for the given load. Belleville disc springs were the most viable option given that their load capacity and travel can be sized independently through washer geometry, stack count, and method of stacking (series and parallel), but stacking enough washers to achieve 2 inches of travel adds significant length to the coupling assembly. Nested wave springs, which combine characteristics from wave and Belleville springs, may be another option. The spring element design is recommended as an area for further development by BWXT engineers.

B. Finite Element Analysis

FEA was performed on the model using Ansys Mechanical to assess whether the coupling could withstand the pressure and temperature loadings it would be subjected to. First, a Steady-State Thermal analysis was performed to compute the temperature distribution in the coupling given the properties of the selected alloy. The thermal gradient between the inside wall of the coupling (exposed to full coolant operating temperature of 900°C) and the outside wall of the coupling (initially modeled as surrounded by air as low as -32°C) produced significant stresses due to dissimilar rates of thermal expansion. Therefore, the results of the Steady-State Thermal analysis were imported into a Static Structural analysis to assess these thermal stresses combined with the mechanical stresses produced by the operating coolant pressure of 4.8 MPa. The allowable stress for the coupling alloy, as supplied by the project client in USCS units, was 4.2 ksi.

Initial results indicated that the coupling would require insulation to reduce heat transfer away from the outer surface of the coupling, thus decreasing the thermal stresses in the material. The radial thickness of the flanges on either end of the coupling showed too large of a temperature change from the inner to outer surfaces, which overly constrained the radial thermal expansion of the coupling and caused stresses exceeding 10 ksi. If the temperature differential across the radius of each flange and along the length of the outer pipe section were constrained to 20°C, the maximum stress in the walls of the coupling dropped to approximately 3.6 ksi, which is comfortably below the material allowable (see Fig. 8). Insulation options need to be investigated further, but ceramic fiber options are promising [21].

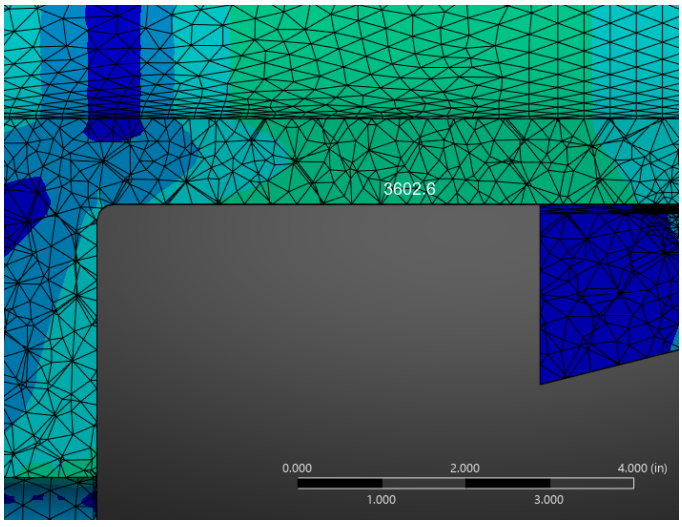

Fig. 8. Maximum stress in the wall of the inner coupling section. Color contours show intervals of 1 ksi, from dark blue (less than 1 ksi) to turquoise (less than 4 ksi).

Additional analysis using the Static Structural module was performed on the lugs that would support the thrust load dissipation system. The maximum stress on the lugs was computed as 0.98 ksi, less than one-fourth of the material allowable for Haynes 230 (4.2 ksi). The location of maximum stress and an exaggerated pattern of deformation are shown in Fig. 9.

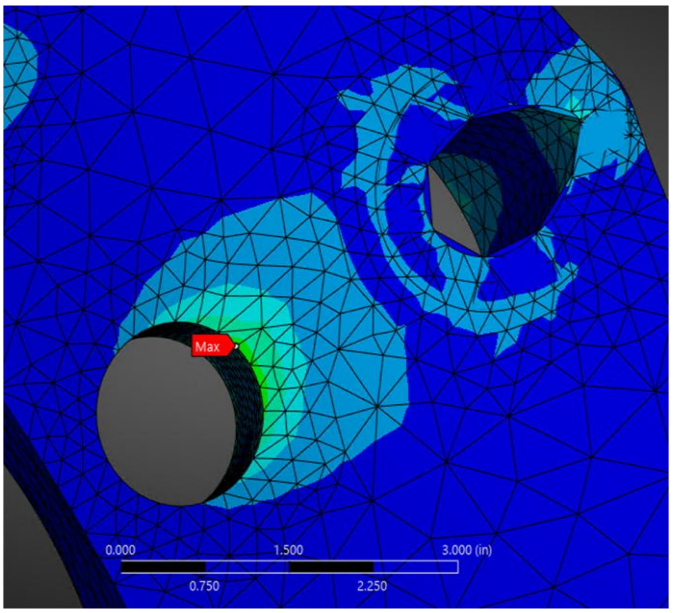

Fig. 9. Lug stresses due to spring system. Color contours occur in intervals of 200 psi (dark blue = up to 200 psi; lime green = up to 1000 psi).

C. Leakage Analysis

Leakage through the TZM seals at full operating temperature and pressure was approximated using an assumed surface roughness as the flow path. Per BWXT, the assumed coolant gas was nitrogen. Detailed theoretical analysis is difficult given the use of a novel sealing mechanism, but an approximate mass flow rate was calculated using:

$$Q = \pi \Delta P h^3 / [6\eta \ln(r_{out}/r_{in})] \quad (2)$$

Here, Q is the volumetric leakage rate (m^3/s), ΔP is the pressure differential across the seal faces (Pa), h^3 is the film thickness/face gap (m), η is the dynamic viscosity of the sealed fluid (Pa-s), r_{in} is the inner radius of the seal face (m), r_{out} is the outer radius of the seal face (m) [22].

For a precision-ground surface finish of Ra 8 µin, the mass flow rate across each seal was estimated as 5 g/day. This exceeds the target of less than 1 g/day but is within the range that BWXT considers acceptable if needed. Further analysis tailored for this application, and possibly Computational Fluid Dynamics (CFD) analysis, will be required.

IV. Discussion

A. Overall Final Model and Improvements

The final result of the team's model was a three-part slip coupling model. The coupling accounts for four inches of extension, meeting the client's requirement. In this model, there are four metallic seals aimed at preventing leaks in the system as well as the inner pipe's expansion. The spring series in the model aim to help counteract the thrust load caused by internal pressure up to 4.8 Mpa on exposed edges inside the coupling, and the tie rods help with stabilization and overextension. A flow piece was incorporated in the final design to decrease pressure drop across the coupling. If more time was allotted to the design process, more iterations of the three-part model would have been developed to further test and refine the design.

B. Analysis results

The results of the FEA performed on the model show promise in meeting the operating requirements of an HTGR primary coolant loop. Insulation using high-temperature materials such as ceramic fiber will be required to mitigate thermal stresses but may require careful design to avoid interfering with the thrust load dissipation system designed to limit the forces the coupling exerts on the surrounding piping.

Additional analysis is also needed to adequately characterize the coupling's performance. For first-of-a-kind components, ASME B31.1 and B31.3 piping direct to the design-by-analysis rules in ASME Boiler & Pressure Vessel Code, Section VIII, Division 2. These rules require a fatigue analysis to prevent failure under cyclic loading. The longevity of the coupling under cyclic loads (in this case, start-up and shutdown of the reactor) has not been assessed.

V. Conclusion

Typical slip couplings currently in production are inadequate for the operating conditions of an HTGR. The proposed coupling design includes metallic seals and an external pressurization element to increase the pressure and temperature performance of the coupling, as well as a spring system to reduce thrust loads on the surrounding piping. Additional analysis is needed to fully characterize the coupling's performance under cyclic loads and further modifications may be necessary to avoid high thermal stresses. However, the design may be a promising new option for high-temperature, high-pressure applications where component size and longevity are of particular concern.

Acknowledgment

The team would like to thank BWXT Advanced Technologies and Sweet Briar College for sponsoring this project. We also thank Michael Staton (BWXT) for supervising this project, as well as Brian Ring and Jonathan Van Heest (BWXT) for additional technical support.

References

[1] H. Wang and X. Zhong, "An overview of high-temperature gas-cooled reactors," in *Nuclear Power Reactor Designs: From History to Advances*, J. Wang, S. Talabi, and S. Bilbao y León, Eds. London, UK:

Academic Press, 2023, pp. 135–162. doi: 10.1016/B978-0-323-99880-2.00008-4.

[2] IAEA, Applicability of Design Safety Requirements to Small Modular Reactor Technologies Intended for Near Term Deployment : Light Water Reactors High Temperature Gas Cooled Reactors. IAEA. [Online]. Available: https://ebookcentral.proquest.com/lib/sbc/detail.action?docID=6482112

[3] "Calculating and Accommodating Thermal Movement in Piping Systems".

[4] "Piping Expansion Joint Design Basics," Flexonics.com. Accessed: Nov. 05, 2025. [Online]. Available: https://flexonics.com/piping-expansion-joint-design-basics/

[5] R. A. Khan, "A Presentation on Expansion Loops," Make Piping Easy. Accessed: Nov. 10, 2025. [Online]. Available: https://makepipingeasy.com/a-presentation-on-expansion-loops/

[6] "What are gimbal expansion joints?," US Bellows. Accessed: Nov. 10, 2025. [Online]. Available: https://usbellows.com/resources/FAQ/what-are-gimbal-expansion-joints/

[7] "Explore Various Types of Metal Expansion Joints & Bellows." Accessed: Nov. 10, 2025. [Online]. Available: https://www.precisionhose.com/products/metal-expansion-joints/types-of-metal-expansion-joints/

[8] "Ball Joint Linkage - Flexible Ball Joint Pipe | Advanced Thermal Systems," Advanced Thermal Systems Inc. Accessed: Nov. 10, 2025. [Online]. Available: https://www.advancedthermal.net/products/ball-joints\

[9] "FLEX-TEND® FLEXIBLE EXPANSION JOINTS, FEATURES AND SPECIFICATIONS." Accessed: Apr. 09, 2026. [Online]. Available: https://ebaa.com/files/pdf/connections/Connections.FT-01.pdf

[10] "Grayloc® Universal Ball Joints | Oceaneering." Accessed: Nov. 10, 2025. [Online]. Available: https://www.oceaneering.com/grayloc-home/grayloc-universal-ball-joints/

[11] "Model R-Pack Packed Slip-Type Expansion Joint," Flexicraft. Accessed: Oct. 29, 2025. [Online]. Available:

[12] "The Difference Between PTFE and Graphite Braided Packing | CRC Distribution." Accessed: Nov. 10, 2025. [Online]. Available: https://resources.crconline.com/difference-between-ptfe-and-graphite-braided-packing

[13] ASME B31.1 - Power Piping, 2024.

[14] "HAYNES® 230®," Haynes International, Mar. 03, 2025. https://haynesintl.com/en/alloys/alloy-portfolio/high-temperature-alloys/haynes-230/#physical-properties .

[15] Enerpac, "NPS Nominal Pipe Size Chart (Inches)," Enerpac Blog, Oct. 2020. [Online]. Available: https://blog.enerpac.com/wp-content/uploads/2020/10/NPS-nominal-pipe-size-chart-inches.pdf. [Accessed: Mar. 26, 2026].

[16] HardHat Engineer, "Weld Neck Flange Dimensions - ASME B16.5," HardHat Engineer. [Online]. Available: https://hardhatengineer.com/weld-neck-flange-dimensions/. [Accessed: Mar. 26, 2026].

[17] Rajendra Piping & Fittings, "ANSI/ASME B16.5 Class 900 lb Flanges Dimensions, Price, Weight Chart," *RPF India*. [Online]. Available: https://www.rpfindia.com/ansi-asme-b16-5-class-900-lb-flanges-dimensions-price-weight-chart.html. [Accessed: Mar. 26, 2026].

[18] Qedfusion.org, 2024. https://qedfusion.org/LIB/PROPS/PANOS/moa.html

[19] "TZM Molybdenum Alloy," Vulcan Metal Group, Feb. 05, 2025. https://vulcanmetalgroup.com/molybdenum-tzm/

[20] "Slip Expansion Joint | Sleeve Expansion Joint | Dresser® Style." Accessed: Mar. 26, 2026. [Online]. Available: http://www.pipingpipeline.com/slip-ej-sleeve-ej.html

[21] "Cerablanket and Cerachem Blankets," Morgan Advanced Materials, Jan. 01, 2025. [Online]. Available: https://www.morganthermalceramics.com/media/drsnyuxw/cerablanket_cerchem-blankets_eng.pdf

[22] Todd, "How to Calculate the Leakage Rate of a Mechanical Seal," Cowseal, Jul. 17, 2025. https://cowseal.com/calculate-leakage-rate-of-mechanical-seal/